

# Geophysical Research Letters<sup>®</sup>



## RESEARCH LETTER

10.1029/2024GL108600

## Mars Soil Temperature and Thermal Properties From InSight HP<sup>3</sup> Data

### Key Points:

- We measured the temperature and its diurnal and annual variations in the top 40 cm of the Martian soil at the InSight landing site
- The soil thermal diffusivity was calculated from the diurnal and seasonal surface and soil temperature variations
- The soil temperature allows the formation of thin films of brine; their efflorescence may explain the formation of the observed duricrust

### Supporting Information:

Supporting Information may be found in the online version of this article.

### Correspondence to:










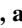


T. Spohn,  
tilman.spohn@dlr.de

### Citation:

Spohn, T., Müller, N., Knollenberg, J., Grott, M., Golombek, M. P., Plesa, A.-C., et al. (2024). Mars soil temperature and thermal properties from InSight HP<sup>3</sup> data. *Geophysical Research Letters*, 51, e2024GL108600. <https://doi.org/10.1029/2024GL108600>

Received 30 JAN 2024

Accepted 13 SEP 2024

T. Spohn<sup>1</sup> , N. Müller<sup>1</sup> , J. Knollenberg<sup>1</sup> , M. Grott<sup>1</sup> , M. P. Golombek<sup>2</sup> , A.-C. Plesa<sup>1</sup> , V. T. Bickel<sup>3</sup> , P. Morgan<sup>4</sup> , C. Krause<sup>5</sup> , D. Breuer<sup>1</sup> , S. E. Smrekar<sup>2</sup> , and W. B. Banerdt<sup>2,6</sup> 

<sup>1</sup>Institute of Planetary Research, German Aerospace Center DLR, Berlin, Germany, <sup>2</sup>Jet Propulsion Laboratory, California Institute of Technology, Pasadena, CA, USA, <sup>3</sup>Center for Space and Habitability, University of Bern, Bern, Switzerland, <sup>4</sup>Colorado Geological Survey, Colorado School of Mines, Golden, CO, USA, <sup>5</sup>MUSC Space Operations and Astronaut Training, German Aerospace Center DLR, Köln, Germany, <sup>6</sup>Retired, Pittsburg, PA, USA

**Abstract** Diurnal and seasonal variations in soil and surface temperature measured with the HP<sup>3</sup> thermal probe and radiometer of NASA's InSight Mars mission are reported. At a representative depth of 10–20 cm, an average temperature of 217.5 K was found, varying by 5.3–6.7 K during a sol and by 13.3 K during the seasons. From the damping of the temperature variation with depth and the phase shift, a thermal diffusivity of  $(3.93 \pm 0.39) \times 10^{-8} \text{ m}^2/\text{s}$  was derived for the upper ~10 cm from the diurnal temperature variation and of  $(3.63 \pm 0.53) \times 10^{-8} \text{ m}^2/\text{s}$  for the ~40 cm depth range of the mole from the annual temperature variation. Using published thermal conductivity and inertia values together with the diffusivities, soil densities of 1,470 and 1,730 kg/m<sup>3</sup> were derived for these depths. The temperatures allow the deliquescence of thin films of brine, the efflorescence of which may explain the cemented duricrust observed.

**Plain Language Summary** Temperature is an important factor in understanding the physical properties of Martian soil. It determines how quickly physical processes and chemical reactions occur, including the transport of heat and materials. Temperature is crucial to astrobiology because it affects the habitability of the soil and the potential for water or brine to support microbial life. We measured the temperature in the soil during several Martian days and over a Martian year using the NASA InSight Mars mission's Heat Flow and Physical Properties Package. The average temperature was  $-56^\circ\text{C}$  (217.5 K) over the depth extent of the thermal probe, which was about 40 cm. The temperature varied by 5–7° during the day, which is only a tenth of the daily surface temperature variation. It varied by 13° during the seasons. The temperature is subfreezing for water, but it allows the formation of thin films of salty brine for 10 hr or more during a Martian day. The solidification of the brine is a likely explanation for the observed few tens of centimeters thick duricrust, a layer of consolidated, cohesive sand, which is thought to have hampered the penetration to greater depth of the mission's thermal probe.

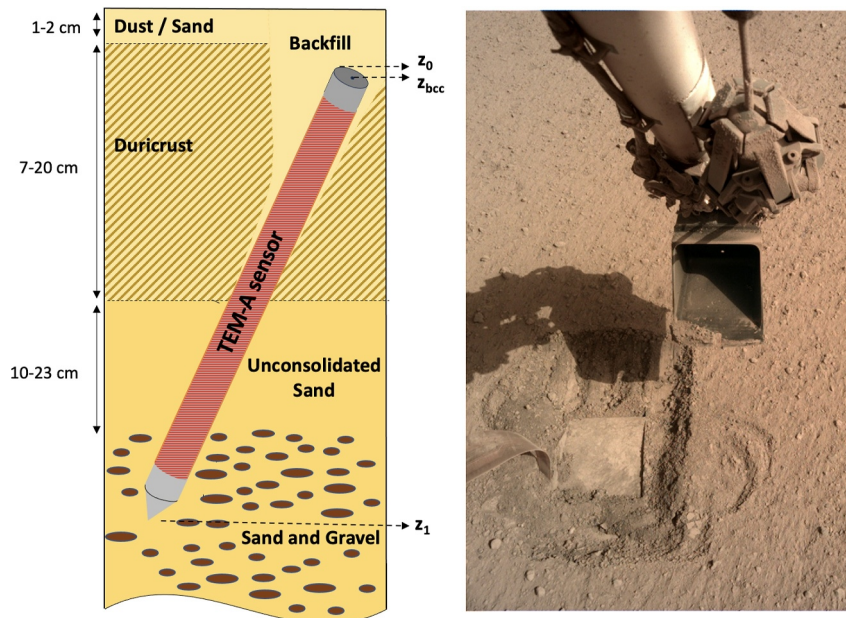
## 1. Introduction

Although the Phoenix lander thermal and electrical conductivity probe measured the near-surface soil temperature at 1.5 cm depth (Zent et al., 2010), the temperature below that has not yet been measured. Soil temperature controls physical properties such as elasticity, seismic velocity, thermal conductivity and heat capacity, which are temperature dependent (e.g., Morgan et al., 2018). Its value and the manner in which it varies in time and space determines the rates and directions of soil physical processes and of energy and mass exchange with deeper layers and the atmosphere (e.g., Hillel, 2001). Moreover, temperature directly controls the rates of chemical reactions that take place in the soil, including potential biological processes. This makes temperature a key factor in astrobiology (e.g., Jones et al., 2011) and future human exploration (e.g., Rapp, 2023).

Soil temperature varies in time and space driven mostly by changes at the surface and the transport of heat in the soil by solid state heat conduction, heat advection through gas transport and latent heat exchange upon for example, freezing and thawing. Heat transport in the Martian soil has been modeled numerous times (e.g., Aharonson & Schorghofer, 2006; Grott et al., 2007; Kieffer, 1976; Mellon et al., 2004) but because of the complex transport processes in the soil and the temperature dependence of material parameters, modeling of the thermal regime can be a formidable task. Here, we report the first measurements of soil temperature at a depth of up to 36 cm using the NASA InSight Mars mission's Heat Flow and Physical Properties Package HP<sup>3</sup>.

© 2024. The Author(s).

This is an open access article under the terms of the [Creative Commons Attribution-NonCommercial-NoDerivs License](https://creativecommons.org/licenses/by/4.0/), which permits use and distribution in any medium, provided the original work is properly cited, the use is non-commercial and no modifications or adaptations are made.



**Figure 1.** Left: Sketch of the mole in the soil and the soil stratigraphy. The red hatching indicates the length of the TEM-A sensor.  $z_0$  is the depth of the topmost edge of the mole that has penetrated at an angle of about  $30^\circ$ .  $z_{bcc}$  is the depth of the center of the back cap.  $z_1$  is the depth of the tip of the mole. The mole pit (right panel) is filled with soil and compacted by the scoop of the robotic Instrument Deployment Arm prior to the sol of the final penetration test.

The InSight mission, a geophysical lander equipped, in addition, with a seismometer, a magnetometer, a meteorology and a radio science package, has been described in detail in for example, Banerdt et al. (2020). The landing site and its geology have been described in Golombek et al. (2020). The lander is located near the equator at  $4.502^\circ\text{N}$ ,  $135.623^\circ\text{E}$  at an elevation of  $-2,613.43$  m with respect to the geoid in an area informally named *Homestead Hollow* in the western Elysium Planitia in the Early Hesperian Transition unit. It is composed of Early Amazonian-Hesperian lava flows with a poorly consolidated, impact-generated 3–17 m thick regolith (Golombek et al., 2020). The data we have collected from this one site on Mars can serve as a valuable reference. The atmospheric and near-surface conditions for InSight are broadly similar to conditions throughout the equatorial region of Mars (within  $\pm 30^\circ$ ). This makes the data representative of about half of the planet's surface.

The HP<sup>3</sup> package was originally planned to measure the planetary surface heat flow and the thermal and mechanical properties of the Martian soil up to 5 m depth (Spohn et al., 2018). Temperature sensors on a 5 m long Kapton<sup>TM</sup> tether would have been brought to the target depth of 3–5 m by a small penetrator, nicknamed the mole. Upon penetration to depth, the thermal conductivity would have been measured at regular depth intervals with a dedicated sensor (TEM-A) on the mole. The 40 cm long mole, which requires friction on its hull to balance remaining recoil from its internal hammer mechanism, did not penetrate to the targeted depth. The root cause of the failure was a lack of friction in an unexpectedly thick cohesive—possibly cemented—duricrust. This was determined through an extensive, almost one Martian year long recovery campaign described in detail in Spohn, Hudson, Witte, et al. (2022) and Spohn, Hudson, Marteau, et al. (2022). The orbital (and surface) thermal inertia at the InSight landing site is low and consistent with unconsolidated fine sand (Golombek et al., 2017, 2020), so strongly cemented duricrust was not expected. During the recovery campaign which ended on sol 754 at the beginning of InSight's second Mars year, the mole's back-end was brought 1–2 cm below the surface, reaching a final tip-depth of about 36 cm with an inclination to vertical of  $30^\circ$ . (A solar day (sol) on Mars is 24 Mars hr of 61.65 min. For InSight, sols are counted starting with the landing on sol 0. A Mars year has 668.58 sols.) Penetration was aided by first gently pushing against the side wall of the mole with the scoop at the end of the robotic Instrument Deployment Arm (Trebi-Ollennu et al., 2018) to increase friction and later by direct support to its back-cap.

The penetration record clearly shows a layering of the soil and its thermo-mechanical properties described in Spohn, Hudson, Marteau, et al. (2022): A 7–20 cm thick duricrust (compare Figure 1) underlies a 1–2 cm sand and

dust layer. The duricrust is followed by a 10–23 cm thick sand layer, then a gravel/sand mixture. The duricrust has a penetration resistance of 0.3–0.7 MPa, while the gravel layer has a resistance of  $4.9 \pm 0.4$  MPa. Using the mole's thermal conductivity sensor TEM-A the average thermal conductivity was measured and the soil density was constrained (Grott et al., 2021). The thermal conductivity for the depth range of the mole was found to be  $0.039 \pm 0.002$  W/m K. This value varies by  $\pm 5\%$  over the seasons (solar longitude between  $8^\circ$  and  $210^\circ$ ) and with atmosphere pressure (Grott et al., 2023).

Prior to each of the seven thermal conductivity measurements in Mars Year 2, we recorded the soil temperature for 48 hr at a cadence of about 15 s using the TEM-A sensor. In addition, housekeeping (H/K) temperature data were taken inside the mole at the motor block at times when the HP<sup>3</sup> instrument was powered on. This occurred at 6:00 and 13:00 local true solar time (LTST), thereby recording diurnal maximum and minimum temperature values on 96 sols during 4/5 of the second InSight Mars year. This paper reports on the diurnal and seasonal variations of the soil temperature and assigns these representative depths. A comparison with the surface temperature measured with the radiometer RAD as part of the HP<sup>3</sup> package (Mueller et al., 2020; Spohn et al., 2018) allows us to calculate the thermal diffusivity of the soil and provide a more precise estimate of the depth of burial of the mole. We can use the thermal diffusivity together with the thermal inertia determined by Piqueux, Mueller, et al. (2021) and the thermal conductivity of Grott et al. (2021) to estimate the soil density.

The mole as a thermal probe and its sensors is described in detail in the Text S1 in Supporting Information S1. It is important to note for the data reported in this paper, that the mole is an extended thermal probe. It was originally designed to measure thermal conductivity using a modified line heat source method (Spohn et al., 2018, 2021, 2023). The length of the mole of about 10 times its diameter is favorable for its use as a modified line heat source probe. The mole hull is made of aluminum of a high thermal conductivity of approximately 200 W/m K, orders of magnitude higher than the expected thermal conductivity of the soil. Other parts of the mole such as the tip are made of mechanically stronger materials of smaller thermal conductivity, but their conductivity is still higher than that of the soil. Thus, the mole is close to isothermal as is illustrated in Figure S3 in Supporting Information S1. Its temperature is measured by the extended, 315 mm long TEM-A sensor (see Figure 1 and Figures S1 and S2 in Supporting Information S1) and the H/K sensor. The TEM-A sensor consists of thin copper wires printed on a Kapton foil whose electrical resistance is temperature dependent and which can be heated for the thermal conductivity measurement. The H/K sensor is a simple thermocouple glued to the mole motor block. The TEM-A sensor is superior to the H/K sensor for measuring the mole temperature, but its operation requires more resources. The readings between the two differ by about a Kelvin at the frequency of the diurnal signal. They differ by only a few tenths of a Kelvin at the annual frequency, for which the H/K sensor readings are used in this paper.

The first 48 hr diurnal soil temperature measurement with the TEM-A thermal sensor on the fully buried mole was taken on sol 680, shortly after burial (Spohn, Hudson, Marteau, et al., 2022) on sol 673, but before the soil was tamped with the robotic arm on sols 686 and 734 as shown in Figure 1. On Sol 754, the mole motor was operated to see if the mole would penetrate further on its own after it was buried and the soil consolidated. When it failed to penetrate significantly during a 506-stroke campaign — the final “Free Mole Test”—attempts to move the mole to a greater depth were abandoned because the diminishing resources were needed for other instruments on the mission. The TEM-A measurement on Sol 795 was the first measurement after the Free Mole Test hammering. This hammering may have contributed to a further settling and compaction of the pit fill. The six subsequent 48hr TEM-A measurements were all taken in the same configuration.

## 2. Results

Figure 2 top panel shows the soil temperature as a function of LTST and for sols 681–1202. The temperature curves are nearly parallel except for sol 681. The smaller amplitude of the diurnal temperature variation was at least partly caused by lower insolation. InSight ICC images (<https://mars.nasa.gov/insight/multimedia/raw-images>, see also Lemmon et al. (2015)) suggest that 681 was a particularly dusty sol at Homestead Hollow. The condition of the soil prior to the “Free Mole Test” and the final tamping of the sand scraped into the pit may have contributed to the anomaly. A more loosely packed sand would be expected to have a lower thermal diffusivity and would attenuate the temperature signal more. The low rate of temperature increase after noon was probably caused by the shadow of the scoop, which was just above the mole at that time. The arm was removed from the vicinity of HP<sup>3</sup> after the “Free Mole Test” to be used with other soil science experiments (e.g., Delage et al., 2024).

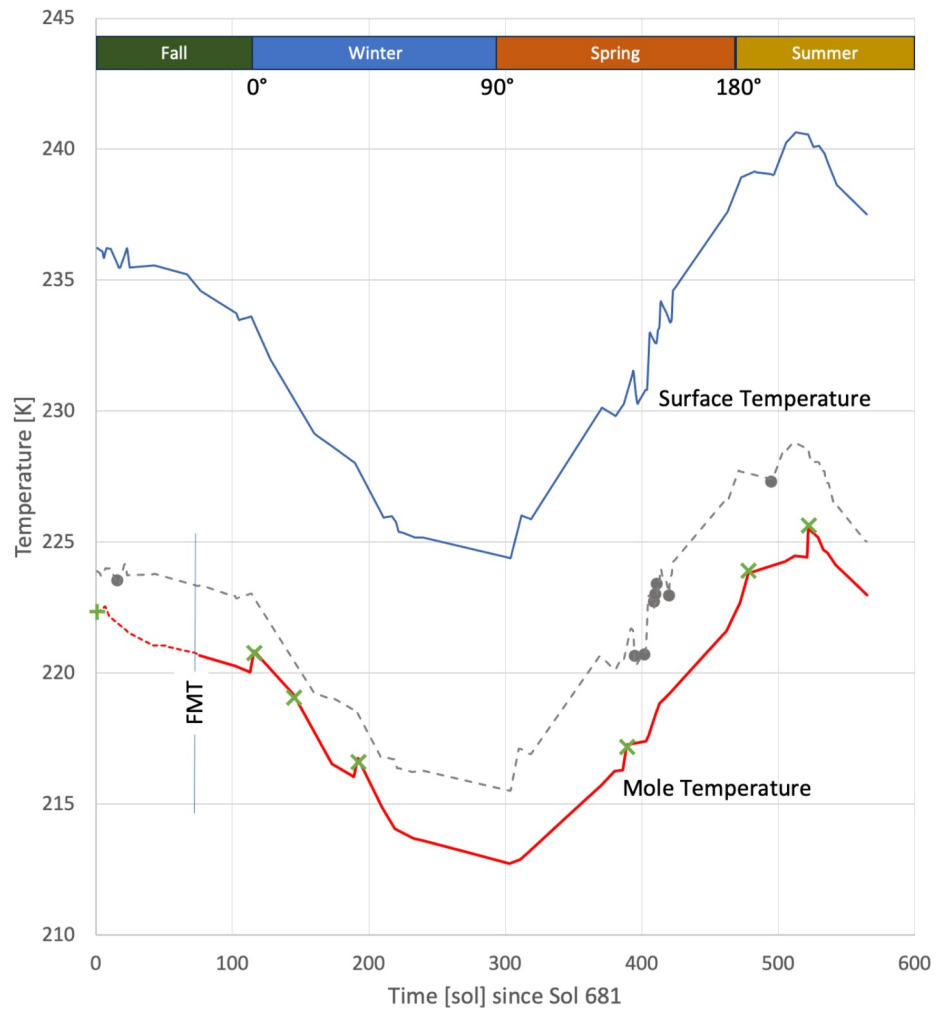
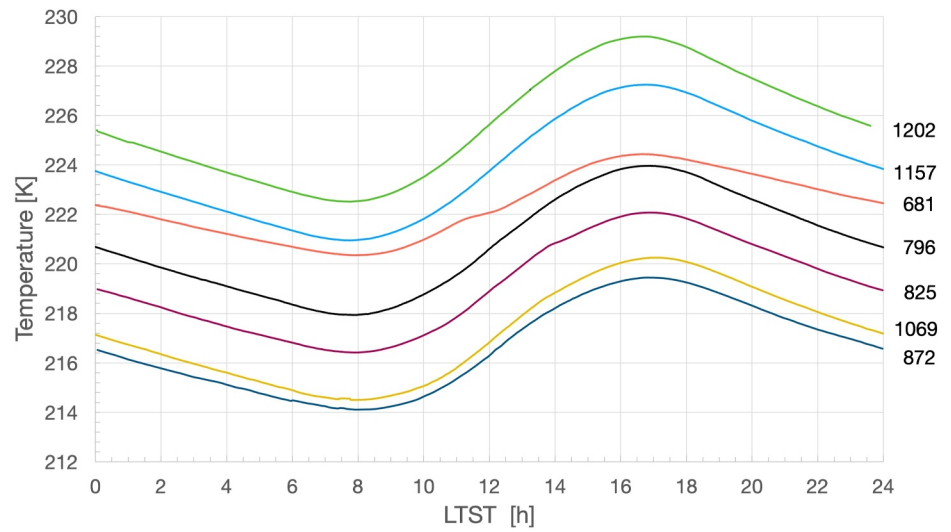


Figure 2.

Figure 2 bottom panel shows the diurnally averaged TEM-A and mole motor housekeeping (H/K) temperature values as a function of time in sols starting at sol 681 and extending to sol 1245, the last sol on which HP<sup>3</sup> data were taken. In addition, we plot the average of the diurnal peak values of the surface temperature measured by the RAD sensor at surface spot2 (cf. Text S1 in Supporting Information S1). Spot2 is located opposite to the location of the mole with respect to the lander, and is centered at a distance of approximately 4 m from the center of the lander. The surface temperature was recorded during the second InSight Mars year at 6:00 and 13:00 LTST, covering the daily maximum and minimum values. The values plotted in Figure 2 are the averages between the two. We also plot the 24-hr average surface temperature for 7 sols of data, along with an estimate of the average surface temperature calculated from the 6:00 and 13:00 LTST values and using a relation between the 24-hr average temperature and the average between the peak-to-trough values derived from InSight Year 1 data. The two curves differ significantly in amplitude, by 8 K in winter and by 13 K in summer, but not in phase. The difference is due to the non-symmetry of the surface temperature variation during a sol (see Figure S5 in the Supporting Information S1). The temperature difference between the hottest day on the Martian surface and the coldest, based on averaging the daily maximum and minimum temperatures, was found to be 16.3 K with an estimated uncertainty of 1 K.

Single-sol temperature in the soil varied by 5.3 K for the coldest sol sampled, sol 871, and by 6.7 K for the warmest sol, sol 1202. Over the seasons, the 24-hr average TEM-A temperatures varied by 9 K from 216.8 K at sol 871 to 225.8 K at sol 1202. Note that the TEM-A measurements missed the temperature low around sol 980 (211.8 K at sol 981, Figure 2 bottom), suggesting a temperature difference through the Martian year of 13.3 K. The annual mean temperature calculated from the TEM-A data and the H/K data is 217.5 K. The annual mean surface temperature is 221.6 K.

The damping of the diurnal and annual surface temperature variation and the phase shift with increasing depth can be used to estimate the thermal diffusivity and the depth to the back-end of the mole. Note that the latter was not well known but was estimated to be 1–2 cm from camera data (Spohn, Hudson, Marteau, et al., 2022). We briefly describe our calculation here. More detail can be found in the Text S2 in Supporting Information S1.

The peak-to-trough temperature variation in a half-space periodically heated at the surface decreases with  $\exp(-z/\delta)$ , where  $z$  is the depth and where  $\delta = \sqrt{\kappa P/\pi}$  is the thermal skin depth, with  $\kappa$  the thermal diffusivity and  $P$  the period of the forcing temperature variation (e.g., Carslaw & Jaeger, 1959). Extensive modeling of the mole as a thermal probe with the HP<sup>3</sup> Thermal Mathematical Model has shown that the mole is an excellent sensor of the soil temperature averaged over the depth of the mole at the annual frequency. At the diurnal frequency, the averaging is somewhat biased toward higher amplitudes and a greater phase shift. More specifically, the ratio between the peak-to-trough variation at depth and at the surface,  $\chi_d$ , of the first harmonic of the diurnal oscillation obeys the following relation

$$\ln \chi_d = -(1.121 \pm 0.020) \phi_d + \ln \frac{\delta_d}{(z_1 - z_0)} + (0.827 \pm 0.032) \quad (1)$$

where the subscript  $d$  refers to the diurnal wave,  $z_0$  is the depth to the back-end of the mole (see Figure 1) and  $z_1$  the depth to the tip of the mole.  $(z_1 - z_0)$  equals the known length of the mole of 40 cm times the cosine of its inclination to vertical of  $30 \pm 2^\circ$ . The phase lag  $\phi_d$  of the temperature variation follows

$$\phi_d = (0.953 \pm 0.016) \frac{z_0}{\delta_d} + (0.907 \pm 0.013) \quad (2)$$

Equations 1 and 2 can be easily inverted for  $z_0$  and  $\delta_d$ , from which  $\kappa$  can be calculated.

**Figure 2.** Top: Soil temperature measured by the TEM-A sensor on the mole as a function of local true solar time (LTST) at the indicated sols (681–1202). Bottom: Surface and mole temperature versus time. The blue line gives the surface temperature averaged from radiometer readings at 6:00 and 13:00 LTST. The gray dots are the available 24-hr averaged surface temperatures. The dashed gray line gives an estimate of the 24-hr average temperature using the diurnal minimum and maximum temperatures from year 2 (blue line) and a mapping derived from the 24-hr averages and peak-to-trough averages from year 1. The green crosses give the mole temperature measured by TEM-A and averaged over one sol. The red line gives the mole temperature averaged from measurements by the H/K sensor at 6:00 and 13:00 LTST. The sol (754) of the “Free Mole Test” is marked with FMT. In addition, the northern hemisphere seasons and the solar longitude are marked.



For the annual wave, because of uncertainty in the amplitude ratio and the difference between the 24-hr and peak-to-trough averages reported above, we use  $z_0$  calculated from the diurnal wave data and the phase shift  $\phi_a$  between the annual surface temperature variation and the temperature variation recorded by the mole sensors

$$\tan \phi_a = \frac{\frac{\sqrt{2}}{2} + e^{-\frac{(z_1 - z_0)}{\delta_a}} + \sin\left(\frac{(z_1 - z_0)}{\delta_a} + \frac{\pi}{4}\right)}{\frac{\sqrt{2}}{2} + e^{-\frac{(z_1 - z_0)}{\delta_a}} + \cos\left(\frac{(z_1 - z_0)}{\delta_a} + \frac{\pi}{4}\right)} \quad (3)$$

where the subscript  $a$  refers to the annual wave. Again,  $\kappa$  is calculated after solving for the skin depth  $\delta_a$ .

For the diurnal wave, we use the six TEM-A 24-hr records available for sols 796–1202 as shown in Figure 2. We compare these with 24-hr surface temperature records from the HP<sup>3</sup> radiometer RAD. Unfortunately, these were not taken on the same sols as the TEM-A records, so we use the next available sol with 24-hr RAD data. These are sol 1075 for sol 1069 and sol 1175 for sol 1157. For sols 796, 825, 872, and 1202, we use data from a nearby sol with a similar solar longitude of the previous Mars year. These are sol 120 (for 796), sol 138 (825), sol 190 (872), and sol 511 (1202). Although InSight's second year on Mars was overall cooler by a few Kelvin than its first, the diurnal temperature variations were very similar.

We find the depth to the top of the mole  $z_0$  to be  $10.2 \pm 1.1$  mm and the thermal diffusivity to be  $(3.93 \pm 0.39) \times 10^{-8} \text{ m}^2 \text{ s}^{-1}$ . Considering the radius of the mole of 13.5 mm and its inclination to the vertical of  $30 \pm 0.2^\circ$ , the center of the back-cap  $z_{bcc}$  is at a depth of  $17 \pm 1.1$  mm. The thermal skin depth is found to be  $33 \pm 1.7$  mm and the wavelength to be 207 mm. The uncertainties of the measurements are detailed in the Text S2 in Supporting Information S1. The uncertainty budget is dominated by the uncertainty in the amplitude ratio  $\chi_d$  of 0.02 and the uncertainty in the third term on the right-hand-side of Equation 1 of 0.032. Following the law of error propagation, the uncertainty in  $\kappa$  is twice the uncertainty in  $\delta_d$ .

The annual wave data are significantly noisier than the diurnal wave records. This is partly a consequence of the weather on Mars and partly due to the smaller and more irregular sampling forced by the dwindling power and manpower resources of the InSight mission. A total of 459 sols (0.69 Martian years) of buried mole data after the “Free Mole Test” with the final hammering (compare Figure 2) are available. The phase shift was determined by performing Fourier analysis on the surface and mole signals. The analysis yielded a phase shift of  $0.196 \pm 0.019$  rad, or  $20.9 \pm 2$  sols. The estimated uncertainty of  $\pm 2$  sols is more conservative than the discretization uncertainty of  $\pm 1.3$  sols. This takes into account the uncertainty in the amplitude, which contributes to the uncertainty in the phase difference. We found the thermal skin depth to be  $82.8 \pm 6.07$  cm,  $\kappa$  to be  $(3.63 \pm 0.532) \times 10^{-8} \text{ m}^2/\text{s}$  and a wavelength of 520 cm. Again, the uncertainty in  $\kappa$  is twice the uncertainty in  $\delta_a$ . The uncertainty in the latter is largely determined by that in the phase shift. (See Supporting Information Text S2 in Supporting Information S1 for details.) A consistency test using the amplitude ratio of the 6:00 and 13:00 LTST averages of the surface and mole signals gave a value for  $\kappa$  of  $(3.71 \pm 2.86) \times 10^{-8} \text{ m}^2/\text{s}$ , close to the value given above but with a much larger uncertainty.

### 3. Discussion and Conclusions

We measured the soil temperature using sensors on the HP<sup>3</sup> mole. By comparing the mole temperature with the surface temperature we find a depth to the center of the mole back-end  $z_{bcc}$  of 1.7 cm using the diurnal thermal wave and a thermal diffusivity of  $(3.93 \pm 0.39) \times 10^{-8} \text{ m}^2/\text{s}$ . Using the annual wave phase data, we find a thermal diffusivity of  $(3.63 \pm 0.532) \times 10^{-8} \text{ m}^2/\text{s}$ . These values are in excellent agreement with the pre-mission estimates of Morgan et al. (2018). Independent estimates of the thickness of the layer over the back-end of the mole from camera data taken during burial and tamping suggest a 1–2 cm thick layer of sand/dust over the mole (Spohn, Hudson, Marteau, et al., 2022), in agreement with the present result.

The average thermal conductivity measured independently by Grott et al. (2021) for the depth range of the mole is  $k = 0.039 \pm 0.002 \text{ W/m K}$ . Zent et al. (2010) report a thermal conductivity for the top 1.5 cm of  $0.085 \text{ W/m K}$  but argue that this value is dominated by heat transport via atmospheric  $\text{CO}_2$ . The thermal inertia derived from the diurnal variation of the surface temperature measured with RAD is  $183 \pm 25 \text{ J/m}^2\text{K s}^{1/2}$ , in agreement with previous data from orbiter measurements (Piqueux, Mueller, et al., 2021). We can use the thermal inertia  $\Gamma$  and the

diffusivity both derived from the diurnal variation of temperature to calculate the thermal conductivity  $k = \Gamma \times \sqrt{\kappa}$  for the depth range of about 2–10 cm, which gives us  $0.036 \pm 0.005$  W/m K. This value is in excellent agreement with the values measured by Presley and Christensen (1997) and consistent with the above value of Grott et al. (2021). It is 15% smaller than the value given by Piqueux, Mueller, et al. (2021), who assumed a sand density of  $1300 \text{ kg/m}^3$ . As a caveat we note that RAD points to a spot on the undisturbed surface, approximately 6 m away from the mole.

The ratio of thermal conductivity to diffusivity gives the heat capacity per unit volume or thermal capacity,  $\rho \times c$ , where  $\rho$  is the soil density and  $c$  is the heat capacity per unit mass. We find that it is about  $10^6 \text{ J/m}^3\text{K}$ , in excellent agreement with the value reported by Zent et al. (2010). The heat capacity per unit volume of terrestrial and meteoritic rocks at room temperature is about  $3 \times 10^6 \text{ J/m}^3\text{K}$  (Szurgot, 2011). This value decreases with density and temperature and reaches about  $10^6 \text{ J/m}^3\text{K}$  at Martian regolith conditions. It has not been possible to measure both  $\rho$  and  $c$  independently and directly for Martian soil. A value of  $1211_{-113}^{+149} \text{ kg/m}^3$  is suggested by Grott et al. (2021) for the soil density from Monte Carlo inversion of their thermal conductivity measurements. However, the spread of their data is large, with values between 900 and  $1800 \text{ kg/m}^3$ .

Morgan et al. (2018) suggest that laboratory values of the heat capacity of lunar basalt soils should be representative of Martian soils as well. Piqueux, Vu, et al. (2021) have substantiated this claim with data on Martian meteorite samples, which vary by about  $\pm 5\%$  between samples in the temperature range of interest. The heat capacity is significantly temperature dependent. A representative value is  $610 \text{ J/kg K}$  for the temperature at mole depth and  $630 \text{ J/kg K}$  at the average surface temperature. The thermal conductivity derived above for the top 10 cm of soil together with the thermal wave diffusivity yields a density of  $1470 \text{ kg/m}^3$ . This density could be representative of the pit fill (see Figure 1). The average depth of the pit is 2 cm and the maximum depth 7 cm (Spohn, Hudson, Marteau, et al., 2022), approximately two diurnal wave thermal skin depths. The width of the pit is approximately two mole radii, which is about the radial distance that the mole disturbs the temperature field (see Figure S3 in Supporting Information S1). The pit fill may be more dense than the duricrust. The sand has been tamped after filling and mole hammering may have settled the grains. The duricrust could still have a density of  $1000\text{--}1200 \text{ kg/m}^3$  as argued by Spohn, Hudson, Marteau, et al. (2022), to explain the formation of the pit.

The annual wave thermal diffusivity and the thermal conductivity value of Grott et al. (2021) yields a density of  $1730 \text{ kg/m}^3$ , with 16% uncertainty, ignoring the uncertainty of the heat capacity. This value is representative of the full depth extent of the mole, along which the density may vary, and is higher than the density cited in Grott et al. (2021) and the density suggested for Martian sand by Morgan et al. (2018). It is consistent with estimates of the density of indurated, blocky Martian soil (Golombek et al., 2008). The density may indicate the presence of a rock component in the soil. A typical basalt density of  $3200 \text{ kg/m}^3$  (e.g., Morgan et al., 2018), yields a rock volume fraction of 15%. This value is consistent with the rock fraction estimate of Spohn, Hudson, Marteau, et al. (2022) based on the thermal conductivity measurement of Grott et al. (2021) and the Martian sand thermal conductivity estimates from Presley and Christensen (1997). Furthermore, it also aligns with the mole penetration record presented in Spohn, Hudson, Marteau, et al. (2022), indicating the presence of gravel, at least at a depth of approximately 30 cm.

A representative average value of the soil temperature is 217.5 K with diurnal variations of about 5–7 K and seasonal variations of about 13 K, respectively. The question is for what depth or range of depths should the estimate be considered representative, given that temperature in the Martian soil generally varies with depth and that the mole thermal sensor measurements provide values averaged over the depth extent of the mole (see Figure S3 in Supporting Information S1). Given that a TEM-A foil is 31.5 cm long and that the tilt of the mole is  $30^\circ$ , its depth extent is 27.3 cm. With a depth to the back-end of the mole in its final configuration of 1.7 cm and a mole length of 40 cm, the tip of the mole is at a depth of 36.3 cm. Since the H/K sensor is at 17.3 cm distance from the back-end, it is at a depth of 16.7 cm below the datum while the center of the TEM-A foil is at 17.7 cm depth. The center of the mole is at a depth of 19.0 cm.

Another way to approach the problem is to consider the attenuation and phase shift of the daily and annual thermal waves and find the depth at which the recorded temperature and its diurnal and annual variations can be expected. By considering the exponential decrease of the peak-to-trough temperature variation and the phase shift increasing with depth, we find for the diurnal wave a representative depth of 9.4 cm. For the annual wave, the observed phase shift gives a representative depth of 16.3 cm. Assuming a Martian surface heat flow of  $20 \text{ mW/m}^2$

(Drilleau et al., 2022; Khan et al., 2021; Plesa et al., 2018) and a thermal conductivity of 0.03–0.04 W/m K, consistent with the present value of  $\kappa$  and Grott et al. (2021), we obtain a thermal gradient of 0.5–0.7 K/m, suggesting a temperature difference between the two representative depths of less than 0.1 K, smaller than the uncertainty range of even the high-quality TEM-A data. We can use the gradient to estimate the temperature increase through the top 5 m of the regolith to obtain a 3–4 K difference from the surface temperature and a bottom temperature of approximately 220 K. This is likely an upper estimate as the thermal conductivity may increase with depth as a consequence of an increasing rock volume concentration (Golombek et al., 2020) which would reduce the temperature increase accordingly.

The above average temperature is about 55 K below the melting temperature of pure ice I and 45 K below the triple point of the “average Mars salinity water” of Jones et al. (2011). It is about 20 K above the H<sub>2</sub>O – Ca(ClO<sub>4</sub>)<sub>2</sub> eutectic and above the average Martian frost point temperature (e.g., Carrozzo et al., 2009). In general, however, estimates of the depth to and the thickness of the cryosphere may need to be revised, as our estimates of the thermal diffusivity are about a factor of two lower than assumed for the near-surface regolith in previous studies (e.g., Clifford et al., 2010). Replacing their thermal conductivity value of 0.06 W/m K with the one calculated here results in an estimated depth to the bottom of the cryosphere that is 150 m less, or 5%.

Jones et al. (2011) discuss a phase space for liquid water on Mars to assess the astrobiological potential of the planet. As an upper estimate for the surface temperature on Mars they use a value of 305 K based on observations from the Opportunity rover at Meridiani Planum. We note that similar values of surface temperature have been observed by HP<sup>3</sup> RAD - for example, 295 K on sol 1202—but that nighttime temperatures have then dropped to values around 200 K and that the temperature in the soil remained well below the freezing temperature of water even in the afternoon (see Figure 2).

Deliquescence of brines in thin films may be more realistic and has been proposed for the Phoenix landing site (e.g., Chevrier et al., 2009; Rennó et al., 2009). For deliquescence to occur, the temperature must be above the eutectic point of the brine and the humidity must be above the deliquescing relative humidity (e.g., Nuding et al., 2014). Thermal conductivity data from Grott et al. (2023) have shown that atmospheric gas diffuses into the soil following surface pressure variations. Pál and Kereszturi (2020) have discussed the potential for deliquescence of three brines, including calcium perchlorate, at Elysium Planitia, the larger region of the InSight landing site. They find about two-hour intervals of favorable temperature conditions for the formation of calcium perchlorate brines at the surface in early spring evenings. Detailed modeling is beyond the scope of this paper, but we note that conditions in the soil at a depth of about 10 cm (and below) would be driven by humidity as the temperature should be continuously above the calcium perchlorate eutectic of about 200 K (Nuding et al., 2014). Judging from the model of Pál and Kereszturi (2020), the brine could be there for hours/sol during winter and spring. This is similar to the finding of Nuding et al. (2014) for the Phoenix landing site, but for a depth of 3 cm, there. At a depth of 3 cm, the time window for deliquescence at Homestead Hollow should be shorter, as the temperature should fall below the eutectic at around 6:00 LTST.

Efflorescence of salt from supersolidus brines may have caused the formation of the approximately 20 cm thick duricrust that impeded the progress of the mole by reducing the friction on its hull as reported in Spohn, Hudson, Witte, et al. (2022) and Spohn, Hudson, Marteau, et al. (2022).

## Data Availability Statement

Calibrated HP<sup>3</sup> radiometer and TEM-A data are archived in NASA's Planetary Data System (InSight HP<sup>3</sup> Science Team, 2021). The specifically selected data, the housekeeping (H/K) sensor data and the Excel workbooks used to evaluate the data have been made publicly available at Spohn (2024).

## References

- Aharonson, O., & Schorghofer, N. (2006). Subsurface ice on Mars with rough topography. *Journal of Geophysical Research*, 111(E11). <https://doi.org/10.1029/2005JE002636>
- Banerdt, W. B., Smrekar, S. E., Banfield, D., Giardini, D., Golombek, M., Johnson, C. L., et al. (2020). Initial results from the InSight mission on Mars. *Nature Geoscience*, 13(3), 183–189. <https://doi.org/10.1038/s41561-020-0544-y>
- Carrozzo, F., Bellucci, G., Altieri, F., D'Aversa, E., & Bibring, J.-P. (2009). Mapping of water frost and ice at low latitudes on Mars. *Icarus*, 203(2), 406–420. <https://doi.org/10.1016/j.icarus.2009.05.020>
- Carlsaw, H. S., & Jaeger, J. (1959). *Conduction of heat in solids* (2nd ed.). Oxford University Press.

## Acknowledgments

We profited from constructive reviews by Ari Koepfel and an anonymous reviewer. The design, building of and research into the HP<sup>3</sup> was supported by the German Aerospace Center DLR, by NASA, the ÖAW, and the Polish Academy of Science. A portion of the work was supported by the InSight Project at the Jet Propulsion Laboratory, California Institute of Technology, under a contract with the National Aeronautics and Space Administration (80NM0018D0004). This is InSight contribution number 337. Open Access funding enabled and organized by Projekt DEAL.



- Chevrier, V. F., Hanley, J., & Altheide, T. S. (2009). Stability of perchlorate hydrates and their liquid solutions at the Phoenix landing site, Mars. *Geophysical Research Letters*, *36*(10). <https://doi.org/10.1029/2009gl0137497>
- Clifford, S. M., Lasue, J., Heggy, E., Boisson, J., McGovern, P., & Max, M. D. (2010). Depth of the Martian cryosphere: Revised estimates and implications for the existence and detection of subpermafrost groundwater. *Journal of Geophysical Research*, *115*(E7). <https://doi.org/10.1029/2009JE003462>
- Delage, P., Caicedo, B., Golombek, M., Spohn, T., Schmelzbach, C., Brinkman, N., et al. (2024). Investigating the Martian soil at the insight landing site. *Soils and Rocks*, *47*(3), e2024005023. <https://doi.org/10.28927/SR.2024.005023>
- Drilleau, M., Samuel, H., Garcia, R. F., Rivoldini, A., Perrin, C., Michaut, C., et al. (2022). Marsquake locations and 1-D seismic models for Mars from InSight data. *Journal of Geophysical Research: Planets*, *127*(9), e2021JE007067. <https://doi.org/10.1029/2021JE007067>
- Golombek, M., Warner, N. H., Grant, J. A., Hauber, E., Ansan, V., Weitz, C. M., et al. (2020). Geology of the InSight landing site on Mars. *Nature Communications*, *11*(1), 1014. <https://doi.org/10.1038/s41467-020-14679-1>
- Golombek, M. P., Haldemann, A. F. C., Simpson, R. A., Fergason, R. L., Putzig, N. E., Arvidson, R. A., et al. (2008). Martian surface properties from joint analysis of orbital, earth-based, and surface observations. In J. F. Bell (Ed.), *The Martian surface: Composition, mineralogy and physical properties* (pp. 468–498). Cambridge University Press. <https://doi.org/10.1017/CBO9780511536076.022>
- Golombek, M. P., Kipp, D., Warner, N. H., Daubar, I. J., Fergason, R., Kirk, R., et al. (2017). Selection of the InSight landing site. *Space Science Reviews*, *211*, 5–95. <https://doi.org/10.1007/s11214-016-0321-9>
- Grott, M., Helbert, J., & Nadalini, R. (2007). Thermal structure of Martian soil and the measurability of the planetary heat flow. *Journal of Geophysical Research (Planets)*, *112*(E9), E09004. <https://doi.org/10.1029/2007JE002905>
- Grott, M., Piqueux, S., Spohn, T., Knollenberg, J., Krause, C., Marteau, E., et al. (2023). Seasonal variations of soil thermal conductivity at the InSight landing site. *Geophysical Research Letters*, *50*(7), e2023GL102975. <https://doi.org/10.1029/2023GL102975>
- Grott, M., Spohn, T., Knollenberg, J., Krause, C., Hudson, T. L., Piqueux, S., et al. (2021). Thermal conductivity of the Martian soil at the InSight landing site from HP<sup>3</sup> active heating experiments. *Journal of Geophysical Research (Planets)*, *126*(7), e06861. <https://doi.org/10.1029/2021JE006861>
- Hillel, D. (2001). Soil physics. In R. A. Meyers (Ed.), *Encyclopedia of physical science and technology 3rd ed, earth sciences* (pp. 77–97). Academic Press.
- InSight HP<sup>3</sup> Science Team. (2021). Mars InSight lander HP<sup>3</sup> data archive [Dataset]. *NASA Planetary Data System*. <https://doi.org/10.17189/1517573>
- Jones, E., Lineweaver, C., & Clarke, J. (2011). An extensive phase space for the potential Martian biosphere. *Astrobiology*, *11*(10), 1017–1033. <https://doi.org/10.1089/ast.2011.0660>
- Khan, A., Ceylan, S., van Driel, M., Giardini, D., Lognonné, P., Samuel, H., et al. (2021). Upper mantle structure of Mars from InSight seismic data. *Science*, *373*(6553), 434–438. <https://doi.org/10.1126/science.abb2966>
- Kieffer, H. H. (1976). Soil and surface temperatures at the Viking landing sites. *Science*, *194*(4271), 1344–1346. <https://doi.org/10.1126/science.194.4271.1344>
- Lemmon, M. T., Wolff, M. J., Bell, J. F., Smith, M. D., Cantor, B. A., & Smith, P. H. (2015). Dust aerosol, clouds, and the atmospheric optical depth record over 5 Mars years of the Mars Exploration Rover mission. *Icarus*, *251*, 96–111. <https://doi.org/10.1016/j.icarus.2014.03.029>
- Mellon, M. T., Feldman, W. C., & Prettyman, T. H. (2004). The presence and stability of ground ice in the southern hemisphere of Mars. *Icarus*, *169*(2), 324–340. <https://doi.org/10.1016/j.icarus.2003.10.022>
- Morgan, P., Grott, M., Knapmeyer-Endrun, B., Golombek, M., Delage, P., Lognonné, P., et al. (2018). A pre-landing assessment of regolith properties at the InSight landing site. *Space Science Reviews*, *214*(6), 104. <https://doi.org/10.1007/s11214-018-0537-y>
- Mueller, N. T., Knollenberg, J., Grott, M., Kopp, E., Walter, I., Krause, C., et al. (2020). Calibration of the HP<sup>3</sup> radiometer on InSight. *Earth and Space Science*, *7*(5), e01086. <https://doi.org/10.1029/2020EA001086>
- Nuding, D., Rivera-Valentin, E., Davis, R., Gough, R., Chevrier, V., & Tolbert, M. (2014). Deliquescence and efflorescence of calcium perchlorate: An investigation of stable aqueous solutions relevant to Mars. *Icarus*, *243*, 420–428. <https://doi.org/10.1016/j.icarus.2014.08.036>
- Pál, B., & Kereszturi, A. (2020). Annual and daily ideal periods for deliquescence at the landing site of InSight based on GCM model calculations. *Icarus*, *340*, 113639. <https://doi.org/10.1016/j.icarus.2020.113639>
- Piqueux, S., Mueller, N., Grott, M., Siegler, M., Millour, E., Forget, F., et al. (2021). Soil thermophysical properties near the InSight Lander derived from 50 sols of radiometer measurements. *Journal of Geophysical Research: Planets*, *126*(11). <https://doi.org/10.1029/2021JE006859>
- Piqueux, S., Vu, T. H., Bapst, J., Garvie, L. A. J., Choukroun, M., & Edwards, C. S. (2021). Specific heat capacity measurements of selected meteorites for planetary surface temperature modeling. *Journal of Geophysical Research: Planets*, *126*(11). <https://doi.org/10.1029/2021JE007003>
- Plesa, A.-C., Padovan, S., Tosi, N., Breuer, D., Grott, M., Wieczorek, M. A., et al. (2018). The thermal state and interior structure of Mars. *Geophysical Research Letters*, *45*(22), 12198–12209. <https://doi.org/10.1029/2018GL080728>
- Presley, M. A., & Christensen, P. R. (1997). The effect of bulk density and particle size sorting on the thermal conductivity of particulate materials under Martian atmospheric pressures. *Journal of Geophysical Research (Planets)*, *102*(E4), 9221–9230. <https://doi.org/10.1029/97JE00271>
- Rapp, D. (2023). *Human missions to mars* (3rd ed.). Springer.
- Renó, N. O., Bos, B. J., Catling, D., Clark, B. C., Drube, L., Fisher, D., et al. (2009). Possible physical and thermodynamical evidence for liquid water at the Phoenix landing site. *Journal of Geophysical Research*, *114*(E1). <https://doi.org/10.1029/2009je003362>
- Spohn, T. (2024). Mars soil temperature and thermal diffusivity from InSight HP<sup>3</sup> data workbook [Dataset, Software]. *FigShare.Collection*. <https://doi.org/10.6084/m9.figshare.25099754>
- Spohn, T., Grott, M., Smrekar, S. E., Knollenberg, J., Hudson, T. L., Krause, C., et al. (2018). The heat flow and physical properties package (HP<sup>3</sup>) for the InSight mission. *Space Science Reviews*, *214*(5), 96. <https://doi.org/10.1007/s11214-018-0531-4>
- Spohn, T., Hudson, T. L., Marteau, E., Golombek, M., Grott, M., Wippermann, T., et al. (2022a). The InSight HP<sup>3</sup> penetrator (Mole) on Mars: Soil properties derived from the penetration attempts and related activities. *Space Science Reviews*, *218*(8), 72. <https://doi.org/10.1007/s11214-022-00941-z>
- Spohn, T., Hudson, T. L., Witte, L., Wippermann, T., Wisniewski, L., Kedziora, B., et al. (2022). The InSight-HP<sup>3</sup> Mole on Mars: Lessons learned from attempts to penetrate to depth in the Martian soil. *Advances in Space Research*, *69*(8), 3140–3163. <https://doi.org/10.1016/j.asr.2022.02.009>
- Szurgot, M. (2011). On the specific heat capacity and thermal capacity of meteorites. In *42nd Lunar and Planetary Science Conference* (Vol. 1150).

- Trebi-Ollennu, A., Kim, W., Ali, K., Khan, O., Sorice, C., Bailey, P., et al. (2018). InSight Mars lander Robotics Instrument Deployment system. *Space Science Reviews*, 214(93), 93. <https://doi.org/10.1007/s11214-018-0520-7>
- Zent, A. P., Hecht, M. H., Cobos, D. R., Wood, S. E., Hudson, T. L., Milkovich, S. M., et al. (2010). Initial results from the thermal and electrical conductivity probe (TECP) on Phoenix. *Journal of Geophysical Research*, 115(E3). <https://doi.org/10.1029/2009JE003420>

### References From the Supporting Information

- Draper, N. R., & Smith, H. (1998). *Applied regression analysis* (p. 706pp). Wiley-Interscience.
- JCGM 100:2008. (2008). *Evaluation of measurement data — Guide to the expression of uncertainty in measurement (GUM)*. Joint Committee for Guides in Metrology. Retrieved from <https://www.iso.org/sites/JCGM/GUM/JCGM100/C045315e-html/C045315e.html?cnumber=50461>